Time-Resolved Charge Translocation by the Ca-ATPase from Sarcoplasmic Reticulum after an ATP Concentration Jump

K. Hartung,* J. P. Froehlich,# and K. Fendler*
*Max-Planck-Institut für Biophysik, Kennedyallee 70, D-60596 Frankfurt/Main, Germany, and #National Institute on Aging, National Institutes of Health, Baltimore, Maryland 21224 USA

ABSTRACT Time-resolved measurements of currents generated by Ca-ATPase from fragmented sarcoplasmic reticulum (SR) are described. SR vesicles spontaneously adsorb to a black lipid membrane acting as a capacitive electrode. Charge translocation by the enzyme is initiated by an ATP concentration jump performed by the light-induced conversion of an inactive precursor (caged ATP) to ATP with a time constant of 2.0 ms at pH 6.2 and 24°C. The shape of the current signal is triphasic, an initial current flow into the vesicle lumen is followed by an outward current and a second slow inward current. The time course of the current signal can be described by five relaxation rate constants, λ_1 to λ_5 plus a fixed delay $D \approx 1$–3 ms. The electrical signal shows that 1) the reaction cycle of the Ca-ATPase contains two electrogenic steps; 2) positive charge is moved toward the luminal side in the first rapid step and toward the cytoplasmic side in the second slow step; 3) at least one electroneutral reaction precedes the electrogenic steps. Relaxation rate constant λ_3 reflects ATP binding, with $\lambda_{3,max} \approx 100\ s^{-1}$. This step is electroneutral. Comparison with the kinetics of the reaction cycle shows that the first electrogenic step (inward current) occurs before the decay of E_2P. Candidates are the formation of phosphoenzyme from E_1ATP ($\lambda_2 \approx 200\ s^{-1}$) and the $E_1P \rightarrow E_2P$ transition ($D \approx 1$ ms or $\lambda_1 \approx 300\ s^{-1}$). The second electrogenic transition (outward current) follows the formation of E_2P ($\lambda_4 \approx 3\ s^{-1}$) and is tentatively assigned to H^+ countertransport after the dissociation of Ca^{2+}. Quenched flow experiments performed under the conditions of the electrical measurements 1) demonstrate competition by caged ATP for ATP-dependent phosphoenzyme formation and 2) yield a rate constant for phosphoenzyme formation of 200 s^{-1}. These results indicate that ATP and caged ATP compete for the substrate binding site, as suggested by the ATP dependence of λ_3 and favor correlation of λ_2 with phosphoenzyme formation.

INTRODUCTION

The Ca-ATPase of the sarcoplasmic reticulum (SR) couples the hydrolysis of ATP to the transport of Ca^{2+} into the SR lumen with a stoichiometry of 2 Ca^{2+}/ATP (for a review see, e.g., De Meis, 1981; Inesi and De Meis, 1985). There is also some evidence that the Ca^{2+} translocation is followed by the countertransport of protons (Chiesi and Inesi, 1980; Levy et al., 1990; Yamaguchi and Kanazawa, 1984, 1985; Inesi and Hill, 1983; Yu et al., 1993, 1994; da Costa and Madeira, 1994). A stoichiometry of 2 Ca^{2+}/x H^+/1 ATP with $x = 1$–3 is consistent with the generation of current by the Ca-ATPase (Hartung et al., 1987; Eisenrauch and Bamberg, 1990). Available data suggest that the Ca^{2+} translocation occurs in at least four steps (Inesi et al., 1990): 1) binding of Ca^{2+} to high affinity sites on the cytoplasmic side of the SR membrane; 2) occlusion of Ca^{2+} bound to the high-affinity sites after the addition of ATP (Sumida and Tonomura, 1974; Dupont, 1980; Takisawa and Makinose, 1981); 3) transfer of Ca^{2+} from high- to low-affinity sites into the SR lumen; and 4) release of Ca^{2+} from the low-affinity sites into the lumen of the SR. The occlusion process on the cytoplasmic surface is relatively fast and probably occurs in parallel to the phosphorylation step (Inesi, 1987; Beeler and Keffer, 1984). Whereas the time course of the slow Ca^{2+} release on the lumenal side could be determined (Beeler and Keffer, 1984; Champeil and Guillain, 1986; Froehlich and Heller, 1985; Inesi, 1987; Khananshvili and Jencks, 1988; Orlowski and Champeil, 1991; Hanel and Jencks, 1991), time-resolved measurements of the occlusion process are impossible with conventional techniques. It seems possible, however, to determine such events with good time resolution if they are coupled to the movement of electrical charge (Fendler et al., 1993).

Recently it has been shown in this laboratory that the Ca-ATPase of the sarcolplasmic reticulum generates an ATP-dependent electrical current (Hartung et al., 1987; Eisenrauch and Bamberg, 1990), confirming earlier suggestions that this transport enzyme is an electrogenic ion pump (Zimniak and Racker, 1978; Beeler, 1980; Navarro and Essig, 1984). Vesicles derived from rabbit SR adsorb spontaneously to a black lipid membrane (BLM) acting as a capacitive electrode. This allows the measurement of time-dependent electrical currents generated by the Ca-ATPase without incorporation of the enzyme into the membrane (Fahr et al., 1981; Borlinghaus et al., 1987). It has been possible to make time-resolved measurements of the pre-steady-state charge translocation by the Ca-ATPase by performing a fast ATP concentration jump, which can be achieved by the laser flash-induced photolysis of caged ATP, a protected analog of ATP (Kaplan et al., 1978). This approach has been used to measure the pre-steady-state charge translocation of the Na-K ATPase (Fendler et al.,

Received for publication 15 October 1996 and in final form 3 March 1997.
Address reprint requests to Dr. Klaus Hartung, Max-Planck-Institut für Biophysik, Kennedyallee 70, D-60596, Frankfurt/Main, Germany. Tel.: 49-69-6303-307; Fax: 49-69-6303-305.

0006-3495/97/06/2503/12 $2.00

1987, 1993; Borlinghaus et al., 1987), the H-K ATPase (Stengelin et al., 1993), and the Kdp-ATPase (Fendler et al., 1996).

The data reported here provide evidence that the reaction cycle of the Ca-ATPase contains at least two electrogenic steps. One electrogenic step is located in the first half of the reaction cycle (i.e., before the decomposition of E_2PCa^{2+}), whereas the second occurs after the formation of E_2PCa^{2+}. It is proposed that positive charge is moved in both transitions. An attempt is made to identify the electrogenic step(s) and to correlate the observed relaxation rate constants with data obtained by other methods, including the chemical quenched flow technique. In addition, the temperature dependence of the charge translocation is described. Some of the experiments have been published in abstract form (Hartung and Fendler, 1989).

MATERIALS AND METHODS

Electrical measurements

Most of the experimental procedure has been described in detail previously (Hartung et al., 1987; see also Fendler et al., 1985, 1987, 1993). Sealed membrane vesicles derived from fragmented sarcoplasmic reticulum (Hasselbach and Makinose, 1963) are adsorbed to a black lipid bilayer (area 1 mm^2) formed in the hole of a septum separating two compartments (volume 1.5 ml) of a Teflon cell. This approach allows the measurement of nonstationary currents generated by the Ca-ATPase by the capacitive coupling between vesicle and supporting membrane (Fahr et al., 1981; Fendler et al., 1987; Borlinghaus et al., 1987; Hartung et al., 1987). Stationary currents can be measured if the supporting membrane is permeabilized with ionophores. Bilayers were made from 1.5% (w/v) diphytanoyl phosphatidylcholine (Avanti Biochemicals, Birmingham, AL) and 0.05% (w/v) octadecylamine (Riedel de Haen, Hannover, Germany) in *n*-decane. The standard electrolyte was (in mM): $CaCl_2$ (1), EGTA (1), $MgCl_2$ (1), dithiothreitol (1), Tris (25). The pH was adjusted with HEPES to 6.2. The free Ca^{2+} concentration was 0.1 mM. The composition of other electrolytes is given in the figure legends. SR vesicles (0.1 mg protein/ml final concentration) and caged ATP were added to the *cis*-compartment of the cuvette (Fig. 1). Current flow across the lipid bilayer is measured by a current to-voltage converter (10^7 V/A, OPA 111; Burr Brown). Voltage measurements were performed with an operational amplifier of high input resistance (10^{13} Ω, OPA 111; Burr Brown). In most experiments the input of the voltage amplifier was shunted by a 10-GΩ resistor. The compartments of the cuvette are connected to the measuring circuit via Ag/AgCl electrodes and agar bridges (2% agar, 100 mM KCl or LiCl). The agar bridges were blackened with ink to avoid photoelectric effects at the Ag/AgCl electrodes. The output of the current-to-voltage converter was amplified (100×), filtered (dc to 300 Hz or dc to 1000 Hz), digitized (Nicolet 2091), and stored on a computer. Light pulses of 308-nm wavelength (10 ns) from an excimer laser (EMG 100; Lambda Physik, Göttingen, Germany) were used to photolyze caged ATP. The maximum energy density in the plane of the membrane was 1.2 J/cm^2. Attenuation of the light intensity was achieved by calibrated neutral density filters covering the UV range (Melles and Griot, Irvine, CA). Standard light pulses (100 mJ/cm^2) photolyzed 17% of the caged ATP near the membrane and 0.3% of the total caged ATP contained in the *cis*-compartment. The fraction of caged ATP photolyzed near the membrane is indicated by η. Higher flash energies could be used at the expense of an increasing risk of destroying the membrane. After each flash, the system was kept in the dark for 10 min and stirred to allow dilution of ATP released by the flash and hydrolysis by enzyme present in the solution. At pH 6.2, 1 mM Mg^{2+}, and 24°C, the time constant for the conversion of caged ATP to ATP is ~2.0 ms (Barabás and Keszthelyi, 1984; Walker et al., 1988). The formation of ATP was determined by the luciferin-luciferase test as described before (Fendler et al., 1985)

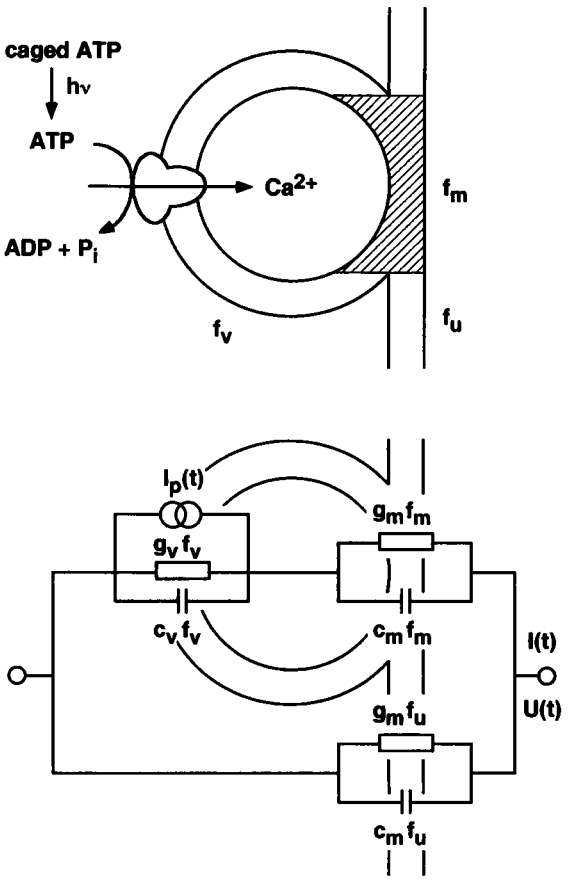

FIGURE 1 Scheme of a SR vesicle adsorbed to a black lipid membrane and its equivalent electrical circuit. f_m, contact area between vesicle and black lipid membrane; f_u, area of the black lipid membrane not covered by vesicles; f_v, area of the vesicle not in contact with the black lipid membrane; $I_p(t)$, current generated by the Ca-ATPase; $I(t)$ and $U(t)$, current and voltage that can be measured; c, specific capacity; g, specific conductance. The subscripts m, v, and u refer to the lipid bilayer, the vesicle, and the uncovered membrane, respectively.

If not indicated otherwise, 1 μM A23187 (Sigma, St. Louis, MO) was added to the *cis*-compartment to prevent Ca^{2+} accumulation inside the vesicles (Scarpa et al., 1972). To measure stationary currents, the protonophore 1799 (kindly provided by Dr. P. Heytler, DuPont Co., Wilmington, DE) was added (Hartung et al., 1987). Free Ca^{2+} and Mg^{2+} concentrations were calculated by an iterative computer algorithm using the stability constants for EGTA and ATP as published by Martell and Smith (1974).

In an attempt to create ATP pulses rather than concentration steps, high concentrations of hexokinase (400 to 1500 units/ml type F-300, Sigma, ST. Louis, MO) and 4 mM glucose were added to the *cis*-compartment. This effectively prevents stationary activity of the enzyme, indicating that most of the ATP released is hydrolyzed within the first turnover of the enzyme.

Quenched-flow measurements

The pre-steady-state time course of phosphoenzyme formation was measured in a multi-mixing apparatus (Froehlich and Taylor, 1975, 1976). Incubation conditions were selected to match those of the bilayer measurements. SR membrane vesicles (0.4–0.8 mg/ml) suspended in a medium containing (in mM) $CaCl_2$ (1), EGTA (1), $MgCl_2$(1), Tris (25), and HEPES (25) (pH 6.2) were mixed with an equal volume of the same solution

containing 0.02–0.4 [γ-^{32}P]ATP and no enzyme, and allowed to incubate for time intervals lasting 4–300 ms. The reaction temperature was maintained at 24°C (Fendler et al., 1993). To terminate the reaction 3% perchloric acid and 6 mM K_2HPO_4 were added from a third syringe, and the protein fraction containing the acid-stable phosphoenzymes was separated from the radiolabeled ATP and inorganic phosphate by centrifugation at 1000 × g at 4°C. The protein washing procedure and assay for [^{32}P]phosphoenzyme were carried out as described (Froehlich and Heller, 1985). Recovery of the protein during the washing procedure was >95%.

Kinetic modeling

The recorded signals were fitted with a model function consisting of a sum of exponentials plus a constant term if a stationary current was present.

An improved fit in the fast rising phase was obtained by introducing a linear time delay D and constraining the function to start at $t = D$, with $I = 0$ and $dI/dt = 0$. This corresponds to a linear, unidirectional, first-order reaction sequence with two ($D = 0$) or more ($D > 0$) electroneutral transitions preceding the electrogenic step. The model function is given by

$$I(t) = \sum_{1}^{4} A_i \exp[-\lambda_i(t - D)] + B \qquad (1a)$$

where, according to the constraints given above, two of the four amplitudes A_i and the stationary current B are not independent fit parameters, but are given by

$$A_1 = -\frac{A_3(\lambda_2 - \lambda_3) + A_4(\lambda_2 - \lambda_4) + B\lambda_2}{\lambda_2 - \lambda_1}$$
$$A_2 = -\frac{A_3(\lambda_1 - \lambda_3) + A_4(\lambda_1 - \lambda_4) + B\lambda_1}{\lambda_1 - \lambda_2} \qquad (1b)$$

This approach reduces the number of fit parameters by 1 and allows one to extract more information out of the fast rising phase of the signal. In the following sections time constants obtained from fit procedures are denoted as relaxation time constants, τ, and the inverse is denoted as a relaxation rate constant, λ, to distinguish it from rate constants describing individual forward and backward reaction steps.

Rate constants for ATP-dependent phosphoenzyme formation in the absence of K^+ were evaluated from the quenched-flow data by fitting to a simple rising exponential function:

$$EP(t) = A[1 - \exp(-kt)]$$

where A is the steady-state level of phosphorylation and k is the apparent rate constant for this reaction. MLAB software (Civilized Software, Bethesda, MD) was used to evaluate these parameters.

RESULTS

Basic properties of the ATP-induced charge translocation

Fig. 2 shows the current signal produced by an ATP concentration jump in the absence of K^+ on three different time scales to demonstrate the different phases of the ATP-induced current. The sign of the current was chosen such that a negative current indicates an inflow of positive charge (Ca^{2+}) into the lumen of the SR vesicle. Immediately after the laser flash a positive current component is observed, which—after a delay—is followed by a negative and a second positive component (Fig. 2 *A*). A second negative component with a very slow time course and small amplitude is visible in signals of large amplitude, as shown in Fig. 2 *C*, which is from a different experiment. The initial positive current after the laser flash is an artefact due to the dissipation of light energy and perhaps photochemical reactions at the surface of the membrane. The very slow negative component is slower than a single turnover of the enzyme. For reasons discussed below, it is assumed to reflect the electrical properties of the combined membrane system (Fig. 1).

The time course of the current signal after the initial artefact can be fitted by a sum of up to five exponential

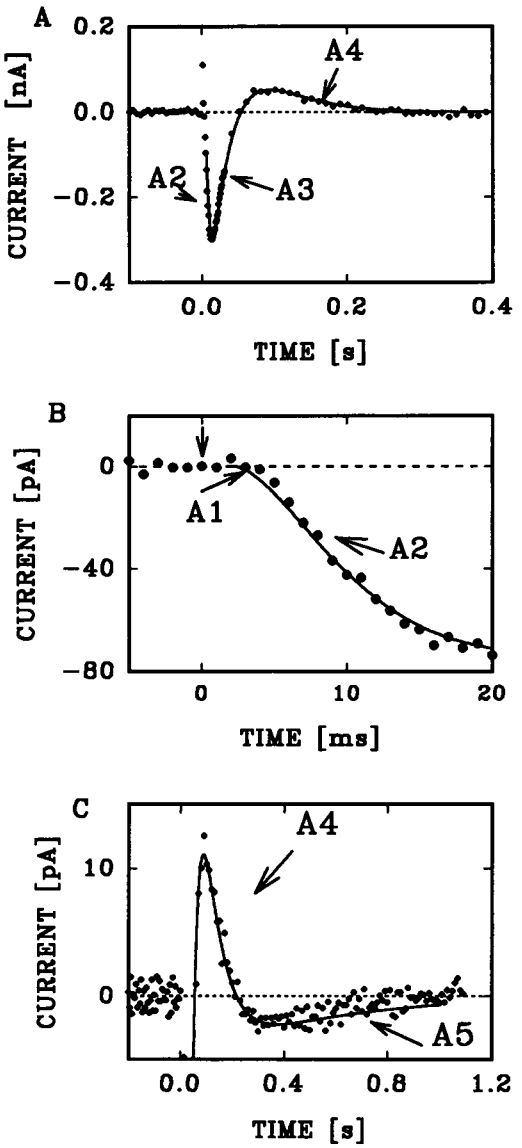

FIGURE 2 Current signal generated by the SR Ca-ATPase after the photolysis of caged ATP by a laser flash. To identify the five components (A_1 to A_5) of the signal, it is plotted with different scalings. *A* and *B* are from the same experiment, but in *B* the intensity of the laser was lower. This allows a better separation between the initial artefact and A_1. *C* is from a different experiment, in which A_5 was clearly visible. Experimental conditions: caged ATP 600 μM (*A*, *B*) and 102 μM (*C*); after the laser flash the concentration of ATP was 29 μM (*A*), 4.8 μM (*B*), or 16 μM (*C*).

functions (A_1 to A_5 with relaxation time constants τ_1 to τ_5; see Fig. 2) and a fixed delay D. In the following the terms, relaxation time constant τ and its inverse the relaxation rate constant $\lambda = 1/\tau$ are used as deemed appropriate. The initial positive component is not fully time resolved at a bandwidth of 1 kHz. Inspection at a larger bandwidth indicates that it lasts for less than 1 ms. Several arguments suggest that it is related to the dissipation of the energy of the laser flash and the release of ATP itself rather than to reactions of the Ca-ATPase: 1) it is observed if caged ATP is photolyzed in the absence of SR vesicles; 2) it is also seen at very low concentrations of Ca^{2+} at which no ATPase activity is expected; 3) saturation with normal ATP (5 mM ATP) prevents the following current signal but not the first positive component. Thus this first current component is an artefact that is not generated by the Ca-ATPase (see also Borlinghaus et al., 1987; Fendler et al., 1987). The following parts of the current signal (A_1 to A_4) behave as expected for a current generated by the Ca-ATPase (see below and Hartung et al., 1987).

ATP dependence of the initial charge translocation

According to the reaction cycle of the Ca-ATPase, the first step after the ATP concentration jump should be binding of ATP to the enzyme. Thus investigation of the ATP dependence of initial charge translocation might help to identify the current components correlated with ATP binding. In principle, there are two possibilities of changing the amount of ATP released per light flash: 1) the concentration of caged ATP may be changed at a constant flash energy and 2) the energy of the laser flash may be varied at a constant concentration of caged ATP. If binding of caged ATP to the ATP binding site is negligible, the two methods should yield identical results. As shown below, this is not the case; caged ATP acts as a competitive inhibitor. Fig. 3 shows the time course of the current signal obtained after a small (2.7 μM) and medium (27 μM) ATP concentration jump. The current signals are superimposed and scaled to the maximum of the negative amplitude to allow comparison of the time course (for details see the figure legend). It is obvious that the initial rising phase is not affected by the 10-fold increase of ATP, whereas the decay is markedly accelerated at the higher ATP concentration. For a detailed analysis, current signals obtained at different concentrations of ATP were fitted with a sum of four exponential functions (A_1 to A_4; see Fig. 2). The ATP dependence of the relaxation rate constants λ_1 to λ_4 is shown in Fig. 4. The relaxation rate constants $\lambda_1 \approx 300\ s^{-1}$, $\lambda_2 \approx 200\ s^{-1}$, and $\lambda_4 \approx 3\ s^{-1}$ are independent of the concentration of ATP. Only λ_3 shows a distinct ATP dependence. It can be described by a Michaelis-Menten formalism with $K = 4.6\ \mu M$. At saturation it is $\lambda_{3,max} = 35\ s^{-1}$ under the conditions of this experiment ($\eta = 0.14$).

In the experiment shown in Figs. 3 and 4, the ATP concentration was modified by the variation of the concentration of caged ATP at constant flash energy. In the same experiment, the concentration of ATP was modified by changing the light intensity ($\eta_{max} = 0.69$) after reaching the final concentration of caged ATP (300 μM). Fig. 5 shows for both conditions the ATP-dependent relaxation rate λ_3 versus the concentration of ATP. It is obvious that saturation of the relaxation rate occurs at much higher ATP concentrations if the ratio of ATP to caged ATP is modified. Half-saturation occurs at 71 μM compared with 4.6 μM,

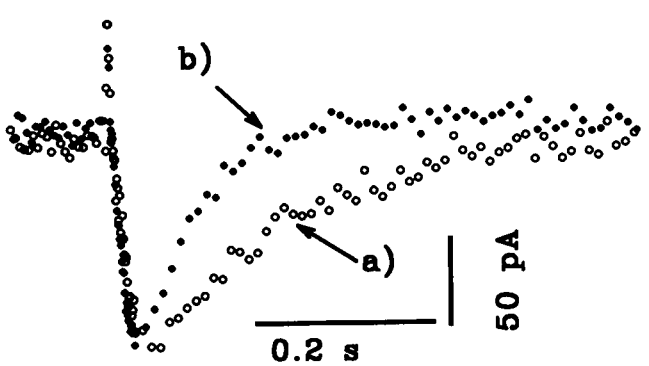

FIGURE 3 Comparison of the ATP-induced current signal after the release of 2.7 (*trace a*) and 27 (*trace b*) μM ATP. Traces are superimposed and scaled to the peak amplitude. Trace *a* has been multiplied by 2.92. The vertical calibration bar refers to trace *b*. The concentration of caged ATP was 20 and 200 μM.

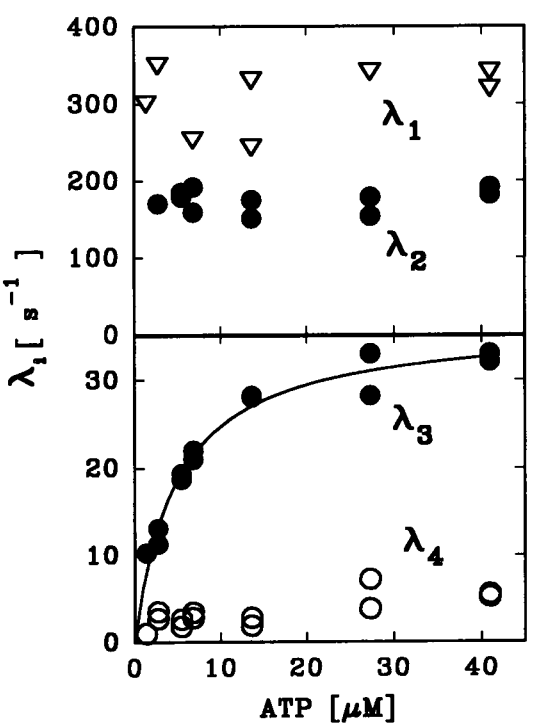

FIGURE 4 ATP dependence of the relaxation rate constants. The amount of ATP released was modified by increasing the concentration of caged ATP while keeping the intensity of the laser flash constant (η = 0.14). Same experiment as in Fig. 3. The ATP dependence of the relaxation rate constant λ_3 was fitted with a Michaelis-Menten-like function with $K_m = 4.6\ \mu M$ and $\lambda_{3,sat} = 35\ s^{-1}$.

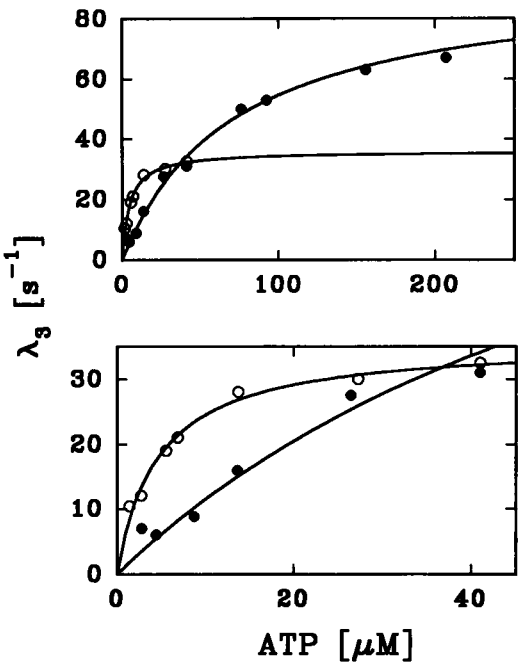

FIGURE 5 The relaxation rate constant λ_3 depends on ATP and caged ATP. In the same experiment the amount of ATP released per flash was first increased by adding increasing amounts of caged ATP at constant energy ($\eta = 0.14$) of the laser flash (○). Then at a concentration of 300 μM caged ATP the amount of ATP released was modified by changing the energy of the laser flash (●), $\eta_{max} = 0.69$). The lower part of the figure shows the data on an expanded scale. Same experiment as in Fig. 3. A Michaelis-Menten equation with $K_m = 4.6$ and 71 μM and $\lambda_{3,max} = 35$ and 94 s^{-1} was fitted to both data sets.

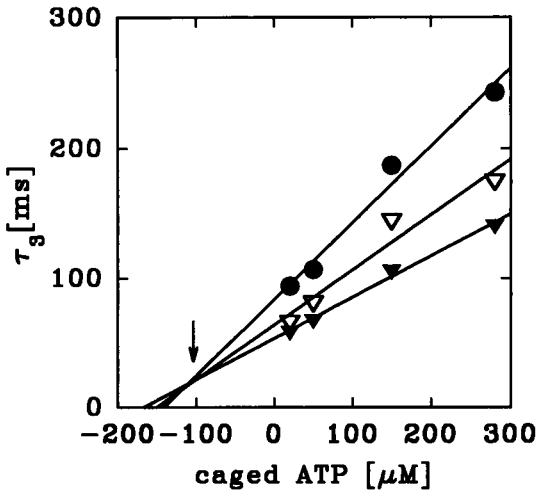

FIGURE 6 Dixon plot of the relaxation time constant τ_3, which was determined at different concentrations of caged ATP and different flash energies. The concentration of caged ATP is that after the laser flash. Data obtained with the same concentration of ATP are denoted by identical symbols and connected by regression lines intersecting at about −100 μM caged ATP, indicating a binding constant of this magnitude. ATP: 1.3 μM (●), 2.4 μM (▽), 5.1 μM (▼).

and $\lambda_{3,max}$ increases from 35 s^{-1} to 94 s^{-1}. The other relaxation rates are unaffected, as shown before in Fig. 4. From this type of experiment it seems clear that caged ATP binds to the Ca-ATPase and affects the kinetics. Qualitatively caged ATP behaves like a competitive inhibitor that is displaced by ATP from the substrate-binding site. To obtain additional quantitative information about the binding of caged ATP to the Ca-ATPase, the ATP dependence of the relaxation rate constant λ_3 was measured at a variety of ratios of ATP to caged ATP. A plot of the ATP-dependent relaxation rate constant at different ATP concentrations versus the caged ATP concentration (Dixon plot) allows one to estimate the binding constant of caged ATP (e.g., Nagel et al., 1987). As shown in Fig. 6, regression lines connecting data points at identical ATP concentrations intersect at about −0.1 mM to −0.15 mM, indicating competitive binding of caged ATP with a binding constant K_i of this magnitude.

Thus it is clear that the relaxation rate constant λ_3 is determined not only by the amount of ATP released, but also by the ratio of caged ATP to ATP. There are, however, two limiting cases that allow one to neglect the exchange reaction. The first is given if the concentration of caged ATP is lower than its binding constant, i.e., [cATP] $\ll K_i$. In the other case, the ATP-binding site must be saturated ([cATP] $\gg K_i$), and the energy of the laser flash should be so high that all caged ATP is photolyzed. We consider the second case first. If caged ATP bound to the ATP-binding site is photolyzed almost completely and no further rearrangement of enzyme and substrate is necessary, then the ATP-dependent component should become very fast. In the limit it should be as fast as the reaction step after ATP binding, i.e., phosphorylation (~200 s^{-1}; see below, Froehlich and Heller, 1985; Petithory and Jencks, 1986), assuming that the photolysis reaction is as fast as in solution (500 s^{-1}) and is not rate limiting. The maximum relaxation rate λ_3 observed experimentally is about 100 s^{-1} if the concentration of caged ATP is 600 μM and about 80% of it is photolyzed in solution. As this is close to 200 s^{-1}, it seems possible that the ATP-dependent reaction is started immediately by the photolysis of caged ATP already bound to the ATP-binding site. The first case ([cATP] = 20 μM $\ll K_i \approx$ 100 μM) is included in Fig. 7, showing the ATP dependence of relaxation rate constant λ_3 at different concentrations of caged ATP and light intensities (same experiment as in Fig. 6). It is obvious that the ATP dependence becomes steeper at decreasing caged ATP concentrations. In the limit [cATP] $\ll K_i$, the ATP binding rate constant may be deduced from the initial slope of the ATP dependence of λ_3. Assuming that this condition holds for 20 μM caged ATP, a binding rate constant of 9×10^6 M^{-1} s^{-1} is obtained from the slope of the relation λ_3 versus ATP at 20 μM cATP. This agrees with binding rate constants obtained by others (Froehlich and Heller, 1985; Froehlich and Taylor, 1975; Fernandez-Belda and Inesi, 1986; Petithory and Jencks, 1988).

Effect of K^+ on the pre-steady-state current

Fig. 8 shows the current signal obtained after the release of ATP in the absence of K^+ (i.e., no K^+ added) and after the

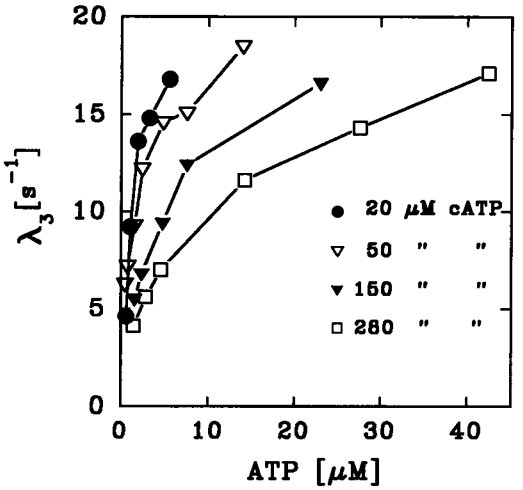

FIGURE 7 Plot of the relaxation rate constant λ_3 versus the ATP concentration at four different concentrations of caged ATP. Concentrations of caged ATP before the flash were 20, 50, 150, and 280 μM. The amount of ATP released at a given concentration of caged ATP was changed by modification of the energy of the laser flash. Same experiment as in Fig. 6.

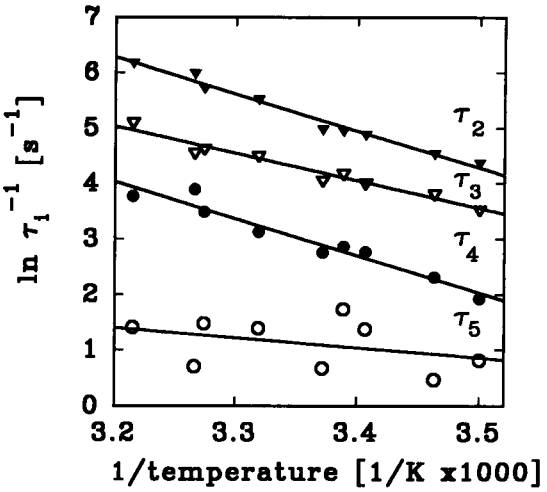

FIGURE 9 Temperature dependence of the relaxation rate constants between 9.6°C and 33.2°C. Current signals were fitted with four exponential functions (i.e., A_1 was neglected). The activation energies were determined from the slopes of the regression lines.

addition of 50 mM K^+ normalized to the same peak amplitude. In the presence of K^+ the amplitude of the signal is reduced by ~50% (see figure legend), but the time course is nearly unchanged. Note that the amplitude of the current obtained in the absence of K^+ has been scaled.

Temperature dependence

The temperature dependence of the ATP-dependent charge translocation has been determined between 9.6°C and 33.2°C. Fig. 9 shows a plot of the relaxation rate constants λ_2, λ_3, λ_4, and λ_5 versus the inverse temperature. The activation energy of the relaxation rate constants λ_2 to λ_4 is between 41 and 55 kJ/mol, which is very similar to that of the peak current, 46 kJ/mol (not shown). The activation energy of the relaxation constant λ_5 is only 15 kJ/mol, suggesting that it is not directly related to the activity of the Ca-ATPase.

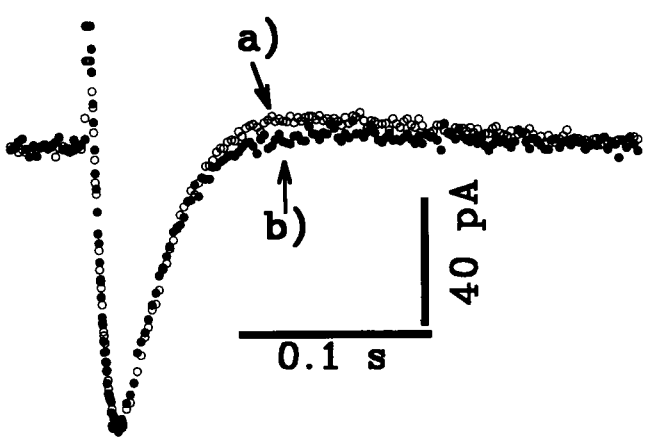

FIGURE 8 Effect of K^+ on pre-steady-state charge translocation. Trace *a* shows the current in the absence of added K^+, and trace *b* the current after the addition of 50 mM K^+. Trace *b* has been scaled by a factor of 1.4. The vertical calibration bar refers to trace *a*. Caged ATP: 600 μM. The ATP concentration after the flash was 55 μM.

The system time constant

The voltage generated by the Ca-ATPase was measured in the presence of K^+ before and after the addition of hexokinase to determine the system time constant from the decay of the voltage after cessation of the activity of the Ca-ATPase. Very high concentrations of hexokinase were used to hydrolyze rapidly the released ATP. This is verified by the disappearance of stationary Ca-ATPase observed with conductive bilayer membranes (Hartung et al., 1987). Fig. 10 shows that before the addition of hexokinase the peak current is followed by a stationary current. After the addition of hexokinase a peak current is still observed, but stationary currents are completely abolished, indicating that most of the ATP released by the laser flash is hydrolyzed during the peak current within ~100 ms.

Fig. 11 shows the voltage generated across the bilayer before and after the addition of hexokinase. In the absence of hexokinase the voltage rises to a stationary level that is maintained for several seconds while a transient behavior is observed in the presence of hexokinase. The decay of the voltage signal in the presence of hexokinase can be described by an exponential function with a time constant of 3 s. Because ATP released by the flash is hydrolyzed much faster (see Fig. 10), it is assumed that the decay of the voltage is determined by the system time constant of the vesicle bilayer combination.

Conductance of vesicles adsorbed to the BLM

It is generally assumed that the SR membrane has a very high conductance between 0.01 and 0.1 S/cm^2 (Hasselbach

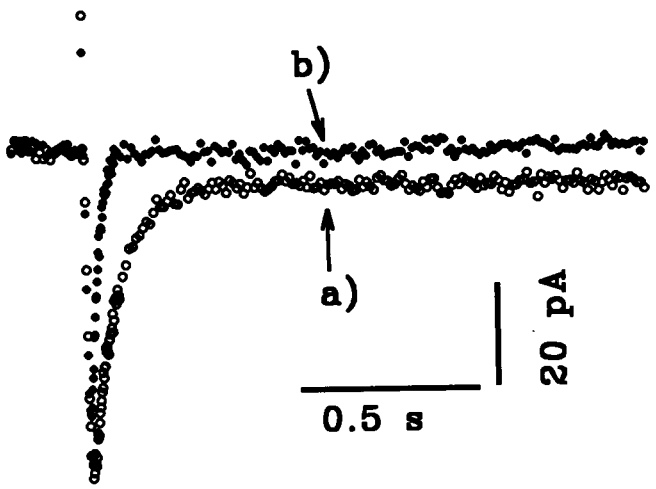

FIGURE 10 Effects of hexokinase and glucose on stationary pump currents. A stationary pump current (*trace a*), which is observed if the supporting bilayer is made permeable with an ionophore (1 μM 1799), disappears if the ATP released is hydrolyzed rapidly by 800 units/ml hexokinase and 2 mM glucose. The membrane conductance was 2.5 nS; the ATP concentration after the flash was 5 μM.

and Oetliker, 1983; Miller et al., 1984). This, however, is in contradiction to a system time constant τ_0 of ~1–3 s as it is derived from the voltage and current measurements described here. In addition, it seems unlikely that such leaky vesicles might create a measurable electrical signal (see Discussion). Therefore, an attempt has been made to determine the electrical conductance of SR vesicles. For this reason the steady-state current has been measured as a function of the overall conductance of the membrane system induced by the protonophore 1799. As shown in the Appendix, the original conductance of the vesicle membrane or at least an upper limit can be deduced from this relation if a number of reasonable assumptions are made.

Fig. 12 shows the relation between the overall conductance and the stationary pump current. The current saturates at ~10 μS/cm^2. Half-saturation occurs at ~1 μS/cm^2. From these data an upper limit of 2 μS/cm^2 for the original conductance of SR vesicles is derived from relations A5 to A7 given in the Appendix. This corresponds to a system time constant $\tau_0 \geq 0.5$ s and agrees with the assumption that τ_5 corresponds to τ_0. It should be noted that the conductance estimated in this way may be too low if the ionophore increases the vesicle conductance much more than that of the BLM. This seems improbable, because practically no measurable stationary current is expected if the vesicle conductance increases much faster than that of the lipid bilayer.

Rapid mixing, quenched-flow experiments

With [γ-^{32}P]ATP as the substrate, rapid mixing, quenched-flow experiments were performed to correlate charge translocation measured with the bilayer technique to the kinetics of phosphoenzyme [EP] formation. The reaction conditions (pH, temperature, ionic composition) were adjusted to coincide with those of the electrical measurements so that a direct comparison could be made between the kinetic results obtained from these experiments.

The ATP dependence of λ_3 (Fig. 4) implies that caged ATP and ATP compete for the same substrate-binding site. This was confirmed in quenched-flow experiments by measuring phosphorylation in the presence and absence of caged ATP (Fig. 13). In these experiments, the total con-

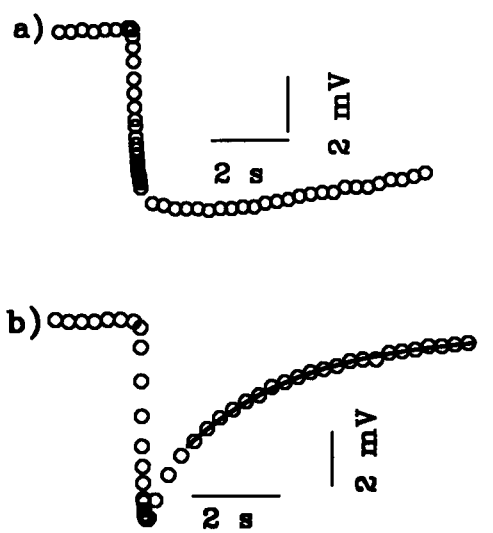

FIGURE 11 Time course of the voltage generated across the bilayer after the release of ATP. Trace *a* shows the signal in the presence of 40 mM K^+ before and after the addition of hexokinase (600 units/ml) and glucose (2 mM). The continuous line fitted to the decay phase represents an exponential function with a time constant of 3.1 s (*trace b*). In these experiments the photolysis of caged ATP was achieved by a flash of 33 ms from a mercury lamp.

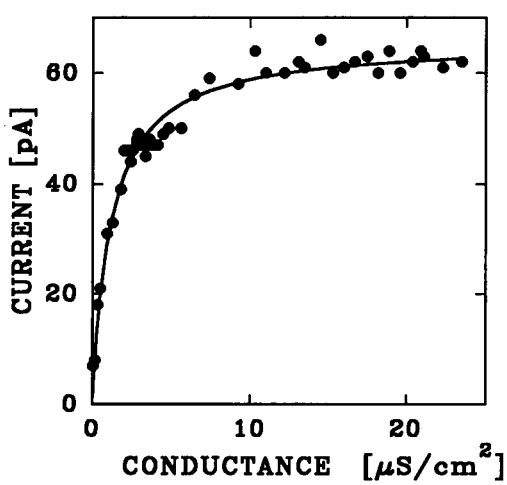

FIGURE 12 Relation between the protonophore induced conductance and the stationary current. The conductance of the vesicle bilayer system was increased by the addition of 8 μM 1799 to both compartments. The conductance and stationary current were determined at different times after the addition of the protonophore. The continuous line is a fit of a Michaelis-Menten equation with an apparent K_m of 1.16 μS/cm^2 to the data points.

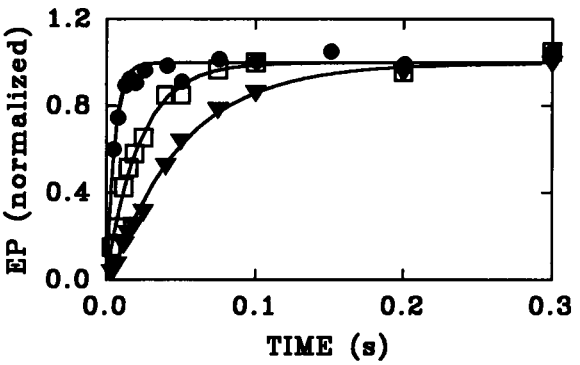

FIGURE 13 Time course of the formation of phosphoenzyme (EP) in the absence of K^+. With 100 μM ATP EP is formed at a rate of 200 s^{-1} (●); with 3.5 μM the rate is 44 s^{-1} (□); and with 3.5 μM ATP and 46.5 μM caged ATP, the rate is 18 s^{-1} (▼). The experimental conditions were the same as for the electrical measurements. See text for details.

centration of nucleotide (ATP + caged ATP) was maintained at 50 μM while the ratio of the ligands was varied. In the absence of K^+, acid-stable phosphoenzyme formation produced by mixing SR membrane vesicles with 3.5 μM ATP obeyed simple exponential kinetics, rising to a stable plateau at a rate of 44 s^{-1} (Fig. 13). To reproduce the conditions of the electrical measurements, enzyme was preincubated with 50 μM caged ATP and then mixed with sufficient ATP and caged ATP to yield final concentrations of 3.5 μM and 46.5 μM, respectively. This corresponds to 7.5% photolytic release of ATP from caged ATP. The addition of caged ATP slowed the apparent rate of phosphorylation to 18 s^{-1}, which is 41% of the control value. When the concentration of ATP was increased to 10 μM (final), representing 25% photolytic release of ATP, caged ATP (40 μM) inhibited the apparent rate of phosphorylation by only 22% (84 versus 107 s^{-1}; data not shown). At both ATP concentrations, the maximum level of phosphorylation was unaffected by the presence of caged ATP.

Between 3.5 and 10 μM ATP the rate of phosphorylation increases, reflecting the fact that the measured rate is an apparent rate constant (k_{app}), which is determined by the second rate constant for ATP binding in the step preceding phosphorylation. To measure the true rate constant for phosphoenzyme formation ($E_1ATP \rightarrow E_1P$), the ATP concentration was increased to 100 μM as shown in Fig. 13. Under these conditions, which are saturating for k_{app} (data not shown), the rate of phosphorylation proceeds at a rate of 208 s^{-1}. This value is similar to the rate of phosphoenzyme formation measured in the presence of K^+ at pH 6.8 (150–200 s^{-1}; Froehlich and Taylor, 1975; Froehlich and Heller, 1985; Petithory and Jencks, 1986), implying that moderate variations in $[K^+]$ and pH do not have strong effects on this reaction. These properties of phosphorylation are consistent with previous results obtained at 2°C (Mahaney et al., 1995).

A bilayer experiment carried out in the presence of 50 μM caged ATP at a laser intensity sufficient to release 2 μM ATP ($\eta = 0.04$) yielded a value for λ_3 of 15 s^{-1}, which is similar to the apparent rate of phosphorylation (k_{app} = 18 s^{-1}) determined by acid quenching under comparable conditions ([caged ATP] = 46.5 μM, [ATP] = 3.5 μM). The approximate agreement between these separately determined kinetic constants implies that the binding competition between ATP and caged ATP at the catalytic site controls the rate of phosphorylation under these conditions.

DISCUSSION

Experimental conditions

Most of the experiments described were performed at pH 6.2 in the absence of potassium at a relatively high concentration of free Ca^{2+} (0.1 mM). This differs from the conditions used by most other investigators and deserves some comment because it complicates comparison with previous work. The low pH was selected to ensure rapid release of ATP from caged ATP (τ = 2.0 ms at pH 6.2, 24°C, but 12 ms at pH 7.0). A high Ca^{2+} concentration was used because it has been shown that the pH dependence of the formation of EP disappears if the concentration of Ca^{2+} is high (0.1 mM; Inesi and Hill, 1983). This pH dependence of phosphorylation reflects competition between Ca^{2+} and H^+ for the Ca^{2+}-binding site, which is suppressed by high $[Ca^{2+}]$. Nominally potassium-free solutions were used because the amplitude of the signal is larger in the absence of K^+. The effect of K^+ on the time course of the signal is negligible (Fig. 8), although it is known that K^+ accelerates the dephosphorylation step (Shigekawa and Dougherty, 1978; Yamada and Ikemoto, 1980). Thus we assume that the pre-steady-state current is determined mostly by intermediates preceding that transition.

At pH 6.2 in the absence of K^+, the rate of phosphorylation was 208 s^{-1} at saturating ATP, comparable to the rates (180–220 s^{-1}) observed in the presence of K^+ at pH 6.8–7.0 (Froehlich and Heller, 1985; Petithory and Jencks, 1986). It is therefore assumed that the data obtained under these conditions are comparable to those obtained under standard conditions, at least with respect to the early steps of the reaction cycle, to which most of the current signal is related.

The intrinsic time constant of the vesicle bilayer system and the conductance of the SR membrane

The black lipid membrane to which the SR vesicles are absorbed acts like a capacitive electrode. The condition of capacitive coupling holds only for times shorter than the electrical time constant of the system adsorbed vesicles-supporting membrane. This and the intention to distinguish it from relaxation processes of the Ca-ATPase make characterization of the electrical time constant a necessity. The following arguments support the idea that the electrical time constant of the supporting membrane plus adsorbed vesicles

is in the range of 1–3 s. In current measurements a component with negative amplitude (A_5, Fig. 2 *C*) has been identified that decays with a time constant $\tau_5 \approx 0.5$–1 s. The activation energy of this component is much lower than that of the other relaxation processes and is of a magnitude expected for a diffusion process. It is assumed that the sign of this component indicates charging of the membrane system due to continous pumping activity. In support of this idea, the sign of this component changes if stationary activity is prevented by the addition of hexokinase. Under these conditions the decay of this component is thought to indicate discharge of the membrane after a single turnover of the enzyme. Voltage measurements that yield a better resolution of slow signal components show that the membrane system discharges with a time constant of ~3 s if the membrane is charged by one cycle of the Ca-ATPase.

Furthermore, the analysis of the relationship between the total conductance of the membrane system and the stationary current indicates a relatively low specific conductance of ~1 μS/cm^2 of the SR membrane. This agrees with the system time constant derived from the current and voltage measurements, but seems to contradict other reports on the conductance of the SR membrane. Estimates of the potassium conductance range from 40 μS/cm^2 to 0.05 S/cm^2, and the chloride conductance may be up to 0.3 S/cm^2 (data collected by Hasselbach and Oetliker, 1983). If this is correct, the time constant τ_0 would be less than a millisecond, far below the time resolution of our recording system.

It can be shown, however, that the discrepancy between previous measurements of the SR conductance and those reported here is apparent. For statistical reasons one may expect that at low channel densities (K^+ channels: 50–100 μm^{-2}, McKinley and Meissner, 1978; Miller et al., 1984; Cl^- channels: <1 μm^{-2}, Hals et al., 1989) and small vesicle size (surface area $\approx$ 0.02 μm^{-2}), a considerable fraction of vesicles are free of channels. Indeed, it has been reported that ~30% of the vesicles do not contain channels (McKinley and Meissner, 1978; Garcia and Miller, 1984). Furthermore, a vesicle with one open channel will have such a high conductance that it is electrically short-circuited and does not contribute to the current signal. In conclusion, we assume that only those vesicles without or with closed ion channels contribute to the current signal. Therefore we do not see a discrepancy between the high overall conductance of the SR membrane reported or postulated and that deduced from our measurements.

Charge translocation in the Ca-ATPase occurs in at least two electrogenic steps

Fig. 2 shows that the current generated by SR vesicles after an ATP concentration jump is first inward, then outward, and then inward again. As discussed before, the late inward current indicates stationary pump activity, whereas the early inward and outward currents discussed now are assigned to the pre-steady-state behavior of the Ca pump. The observation that the current signal begins with zero slope indicates that there is at least one nonelectrogenic step preceding the first charge-translocating transition. The reversal of the direction of current flow during the first cycle after an ATP concentration jump can be explained only if the reaction cycle of the Ca-ATPase contains at least two electrogenic steps. The direction of current flow is compatible with the translocation of positive charge in both steps. In a first rapid step, positive charge is moved toward the lumen of the SR vesicle, and in a second slow step, positive charge is moved toward the cytoplasmic side of the SR vesicle. Because all transitions of the Ca^{2+}-loaded enzyme up to the formation of the E_2P intermediate are fairly rapid, whereas the following reactions are much slower (e.g. Froehlich and Heller, 1985), it seems appropriate to assign the inward current to the Ca^{2+}-loaded form of the enzyme and the outward current to the Ca^{2+}-dissociated form (see the following section for a detailed discussion of this point). Thus one must assume that the Ca-ATPase translocates positive charge throughout the reaction cycle. However, less positive charge must be bound to the Ca^{2+}-dissociated enzyme than to the Ca^{2+}-loaded form (e.g., 1–3 H^+ versus 2 Ca^{2+}); otherwise the constraint of net inward current under stationary conditions would be violated.

It should be noted that similar experiments conducted with Na,K-ATPase (Borlinghaus et al., 1987; Fendler et al., 1987, 1993) and H,K-ATPase (Stengelin et al., 1993) did not provide evidence for more than one electrogenic step, although other experiments suggest that the reaction cycle of both enzymes contains two electrogenic steps (Rakowski et al., 1991; Lorentzon et al., 1988).

The proposal that the Ca^{2+}-loaded ATPase moves positive charge in the same direction in which Ca^{2+} is transported is in contrast to previous reports on another Ca^{2+} transport system, the Na-Ca exchanger, which is negatively charged when loaded with Ca^{2+} (Niggli and Lederer, 1991; Kappl and Hartung, 1996).

Correlation between the relaxation rate constants λ_1 to λ_4 and the reaction cycle

In this section an attempt is made to establish a correlation between the relaxation rate constants λ_1 to λ_4 of the current signal and known reaction steps of the Ca-ATPase reaction cycle. The magnitude of the relaxation rate constants and their assignment to different processes are compiled in Table 1.

Because λ_3 is the only ATP-dependent relaxation rate constant, we must assume that λ_3 describes the binding reaction of ATP to Ca-ATPase. The experiments show, however, that caged ATP competes with ATP such that λ_3 depends on both the ATP and caged ATP concentrations.

The rising phase of the current signal has a sigmoidal shape that can be described by a fixed delay, $D \approx 1$ ms, and two exponential functions, A_1 and A_2, with relaxation rate constants $\lambda_1 \approx 320\ s^{-1}$ and $\lambda_2 \approx 170\ s^{-1}$, respectively. The delay and λ_1 probably contain contributions from various

TABLE 1 Assignment of kinetic parameters to partial reactions of the Ca^{2+}-ATPase reaction cycle

Kinetic parameters		Reaction	Remark
D	1 ms	Caged ATP → ATP	
λ_1	320 s^{-1}	$E_1P \rightarrow E_2P$	1st electrogenic step
λ_2	170 s^{-1}	$E_1ATP \rightarrow E_1P$	1st electrogenic step
λ_3	10–90 s^{-1}	$E_1 \rightarrow E_1ATP$	ATP-dependent
λ_4	4 s^{-1}	$E_2P \rightarrow E_1$	2nd electrogenic step
λ_5	0.3 s^{-1}	τ_0	System time constant

The assignment of the parameters D and λ_1 to the indicated reaction steps is not ambiguous and may be interchanged. It is also not clear which of the reactions indicated performs the first electrogenic transition. It is possible that both transitions are electrogenic.

sources: the filtering time constant (1 ms), release of ATP from caged ATP (400 s^{-1}), and the conformational transition $E_1P \rightarrow E_2P$ (1000 s^{-1}, Froehlich and Heller, 1985). The magnitude of λ_2 correlates very well with the rate of the $E_1ATP \rightarrow E_1P$ + ADP transition (200 s^{-1}, Froehlich and Heller, 1985; Petithory and Jencks, 1986), which itself is closely related to the occlusion of Ca^{2+}. λ_2 is therefore assigned to the $E_1ATPCa^{2+} \rightarrow E_1PCa^{2+}$ + ADP transition.

The relaxation rate constant λ_4, which is independent of ATP, is ~3–5 s^{-1} at pH 6.2 and "0" K^+. Because there is no intermediate with a comparable lifetime in the first part of the reaction cycle, it is assumed that this relaxation rate is related to a transition after the formation of ADP-insensitive phosphoenzyme (E_2P). Reasonable candidates would be dephosphorylation and the release of Ca^{2+} on the luminal side of the vesicle. The latter proceeds at a rate of ~3 s^{-1} under comparable conditions (Champeil and Guillain, 1986; Orlowski and Champeil, 1991). The sign of the amplitude of A_4 indicates, however, current flow in the direction opposite that of Ca^{2+} transport; i.e., although this relaxation may be related to the release of Ca^{2+} it cannot be Ca^{2+} release itself. One possibility is the transport of other cations like protons toward the cytoplasmic side of the vesicles after the release of Ca^{2+} on the luminal side. This idea is supported by reports from several laboratories suggesting that inward transport of Ca^{2+} is followed by an outward movement of protons (Yamaguchi and Kanazawa, 1984, 1985; Inesi and Hill, 1983; Levy et al., 1990; Madeira, 1978; Chiesi and Inesi, 1980; Yu et al., 1993, 1994). A countertransport of protons is, of course, not in contradiction to the observed electrogenicity if fewer than four H^+ are transported per cycle. The slope of the current-voltage relation of SR Ca-ATPase molecules incorporated into black lipid membranes supports the idea that fewer than four electrical charges are moved per cycle (Eisenrauch and Bamberg, 1990).

CONCLUSION

The first part of the reaction cycle contains at least one electrogenic and one preceding nonelectrogenic transition. Reasonable candidates for electrogenic transitions are the formation of E_1P from E_1ATP and the $E_1P \rightarrow E_2P$ transition or both. At present we cannot distinguish between these possibilities. The second electrogenic step occurs after the formation of E_2P and the dissociation of Ca^{2+} and is tentatively assigned to the countertransport of H^+.

APPENDIX

The specific conductances of the vesicle, the lipid bilayer, and the contact area of the vesicle are given by

$$g_i = g_i^0 + g \tag{A1}$$

the respective areas being f_i (see Fig. 1). Here i stands for v, u, and m, which are the vesicle, the uncovered lipid bilayer, and the contact area of the vesicle, respectively. The specific conductance in the absence of ionophore is g_i^0; the specific conductance induced by the ionophores is g. It is is assumed that the ionophores induce the same additional conductivity in all three membranes. Furthermore, the specific conductances in the uncovered lipid bilayer and the contact area are assumed to have the same value ($g_u = g_m$).

The measured conductivity of the total compound membrane G is approximated by

$$G = gF \tag{A2}$$

F is the total membrane area. This approximation is based on the observation that the total conductivity of the compound membrane is much smaller than the conductivity in the presence of ionophore ($g_m^0 \ll g_m$, $g_m \approx g$) and that the conductivity does not change upon addition of the vesicles.

The measured stationary current I_s can be calculated from the current I_p generated by the ion pump using

$$I_s = I_p \frac{f_m g}{f_v(g_v^0 + g) + f_m g} \tag{A3}$$

With Eq. A2 one obtains

$$\frac{I_s}{I_p}\frac{f_m + f_v}{f_m} = \frac{G}{G + G_{0.5}} \tag{A4}$$

with

$$G_{0.5} = \frac{g_v^0 f_v F}{f_m + f_v} \tag{A5}$$

$G_{0.5}$ is the half-saturating conductivity of the stationary current. From Eq. A5 the vesicle conductivity in the absence of ionophores can be calculated in the following limiting cases:

1. $f_m \ll f_v$, i.e., half of the vesicle surface is in contact with the lipid bilayer:

$$g_v^0 = \frac{2G_{0.5}}{F} \tag{A6}$$

2. $f_m \ll f_v$, i.e., only a small part of the vesicle is in contact with the lipid bilayer:

$$g_v^0 = \frac{G_{0.5}}{F} \tag{A7}$$

Relations A6 and A7 are derived under the assumption that the ionophore affects the conductivity of the vesicle membrane in the same way as it does

that of the lipid bilayer. If, however, the ionophore is ineffective in the vesicle membrane, then Eq. A7 holds for case 1, and for case 2 the following relationship is obtained:

$$g_v^0 \ll \frac{G_{0.5}}{F} \quad \text{(A8)}$$

No measurable current I_s would be obtained if both the initial conductance of the vesicle membrane and its increment g were much larger than these values for the lipid bilayer.

The authors thank Prof. E. Bamberg for continuous support, Dr. E. Grell for providing caged ATP, and S. Stolle and E. Harbich for excellent technical assistance.

REFERENCES

Barabás, K., and L. Keszthelyi. 1984. Temperature dependence of ATP release from "caged" ATP. *Acta Biochim. Biophys. Acad. Sci. Hung.* 19:305–309.

Beeler, T. J. 1980. Ca^{2+} uptake and membrane potential in sarcoplasmic reticulum vesicles. *J. Biol. Chem.* 255:9156–9161.

Beeler, T., and J. Keffer. 1984. The rate of Ca^{2+} translocation by sarcoplasmic reticulum (Ca^{2+}-Mg^{2+})-ATPase measured with intravesicular arsenazo III. *Biochim. Biophys. Acta.* 773:99–105.

Borlinghaus, R., H.-J. Apell, and P. Läuger. 1987. Fast charge translocations associated with partial reactions of the Na,K pump. I. Current and voltage transients after photochemical release of ATP. *J. Membr. Biol.* 97:161–178.

Champeil, P., and F. Guillain. 1986. Rapid filtration study of the phosphorylation-dependent dissociation of calcium from transport sites of purified sarcoplasmic reticulum ATPase and ATP modulation of the catalytic cycle. *Biochemistry.* 25:7623–7633.

Chiesi, M., and G. Inesi. 1980. Adenosine 5′-triphosphate dependent fluxes of manganese and hydrogen ions in sarcoplasmic reticulum vesicles. *Biochemistry.* 19:2912–2918.

da Costa, A. G., and V. M. Madeira. 1994. Proton ejection as a major feature of the Ca^{2+} pump. *Biochim. Biophys. Acta.* 1189:181–188.

De Meis, L. 1981. The Sarcoplasmic Reticulum. John Wiley, New York.

Dupont, Y. 1980. Occlusion of divalent cations in the phosphorylated calcium pump of sarcoplasmic reticulum. *Eur. J. Biochem.* 109: 231–238.

Eisenrauch, A., and E. Bamberg. 1990. Voltage-dependent pump-currents of the sarcoplasmic reticulum Ca^{2+}-ATPase in planar lipid membranes. *FEBS Lett.* 268:152–156.

Fahr, A., P. Läuger, and E. Bamberg. 1981. Photocurrent kinetics of purple-membrane sheets bound to planar bilayer membranes. *J. Membr. Biol.* 60:51–62.

Fendler, K., S. Dröse, K. Altendorf, and E. Bamberg. 1996. Electrogenic K^+ transport by the Kdp-ATPase of *Escherichia coli*. *Biochemistry.* 35:8009–8017.

Fendler, K., E. Grell, and E. Bamberg. 1987. Kinetics of pump currents generated by the Na^+,K^+-ATPase. *FEBS Lett.* 24:83–88.

Fendler, K., E. Grell, M. Haubs, and E. Bamberg. 1985. Pump currents generated by the purified Na^+K^+-ATPase from kidney on black lipid membranes. *EMBO J.* 4:3079–3085.

Fendler, K., S. Jaruschewski, A. Hobbs, W. Albers, and J. P. Froehlich. 1993. Pre-steady-state charge translocation in NaK-ATPase from eel electric organ. *J. Gen. Physiol.* 102:631–666.

Fernandez-Belda, F., and G. Inesi. 1986. Transmembrane gradient and ligand-induced mechanisms of adenosine 5′-triphosphate synthesis by sarcoplasmic reticulum adenosine triphosphatase. *Biochemistry.* 25: 8083–8089.

Froehlich, J. P., and P. F. Heller. 1985. Transient-state kinetics of the ADP-insensitive phosphoenzyme in sarcoplasmic reticulum: implications for transient-state calcium translocation. *Biochemistry.* 24: 126–136.

Froehlich, J. P., and E. W. Taylor. 1975. Transient state kinetic studies of sarcoplasmic reticulum adenosine triphosphatase. *J. Biol. Chem.* 250: 2013–2021.

Froehlich, J. P., and E. W. Taylor. 1976. Transient state kinetic effects of calcium ions on sarcoplasmic reticulum adenosine triphosphatase. *J. Biol. Chem.* 251:2307–2315.

Garcia, A. M., and C. Miller. 1984. Channel-mediated monovalent cation fluxes in isolated sarcoplasmic reticulum vesicles. *J. Gen. Physiol.* 83:819–839.

Hals, G. D., P. G. Stein, and P. T. Palade. 1989. Single channel characteristics of a high conductance anion channel in "sarcoballs." *J. Gen. Physiol.* 93:385–410.

Hanel, A. M., and W. P. Jencks. 1991. Dissociation of calcium from the phosphorylated calcium-transporting adenosine triphosphatase of sarcoplasmic reticulum: kinetic equivalence of the calcium ions bound to the phosphorylated enzyme. *Biochemistry.* 30:11320–11330.

Hartung, K., and K. Fendler. 1989. Charge translocation by the sarcoplasmic Ca ATPase after an ATP concentration jump. *J. Protein Chem.* 8:377–378.

Hartung, K., E. Grell, W. Hasselbach, and E. Bamberg. 1987. Electrical pump currents generated by the Ca^{2+}-ATPase of sarcoplasmic reticulum vesicles adsorbed on black lipid membranes. *Biochim. Biophys. Acta.* 900:209–220.

Hasselbach, W., and M. Makinose. 1963. Über den Mechanismus des Calciumtransportes durch die Membranen des sarkoplasmatischen Retikulums. *Biochem. Z.* 339:94–111.

Hasselbach, W., and H. Oetliker. 1983. Energetics and electrogenicity of the sarcoplasmic reticulum calcium pump. *Annu. Rev. Physiol.* 45: 325–339.

Inesi, G. 1987. Sequential mechanism of calcium binding and translocation in sarcoplasmic reticulum adenosine triphosphatase. *J. Biol. Chem.* 262:16338–16342.

Inesi, G., and T. L. Hill. 1983. Calcium and proton dependence of sarcoplasmic reticulum ATPase. *Biophys. J.* 44:271–280.

Inesi, G., and L. De Meis. 1985. Kinetic regulation of catalytic and transport activities in sarcoplasmic reticulum ATPase. *In* The Enzymes of Biological Membranes, Vol. 3, 2nd Ed. A. N. Martonosi, editor. Plenum Press, New York. 157–191.

Inesi, G., C. Sumbilla, and M. E. Kirtley. 1990. Relationships of molecular structure and function in Ca^{2+}-transport ATPase. *Physiol. Rev.* 70: 749–760.

Kaplan, J. H., B. Forbush III, and J. F. Hoffmann. 1978. Rapid photolytic release of adenosine 5′-triphosphate from a protected analogue: utilization by the Na:K pump of human red cell ghosts. *Biochemistry.* 17: 1929–1935.

Kappl, M., and K. Hartung. 1996. Rapid charge translocation by the Na^+-Ca^{2+} exchanger after a Ca^{2+} concentration jump. *Biophys. J.* 71:2473–2485.

Khananshvili, D., and W. P. Jencks. 1988. Two step internalization of Ca^{2+} from a single E~P·Ca_2 species by the Ca^{2+}-ATPase. *Biochemistry.* 27:2943–2952.

Levy, D., M. Seigneuret, A. Bluzat, and J.-L. Rigaud. 1990. Evidence for proton countertransport by the sarcoplasmic reticulum Ca^{2+}-ATPase during calcium transport in reconstituted proteoliposomes with low ionic permeability. *J. Biol. Chem.* 265:19524–19534.

Lorentzon, P., G. Sachs, and B. Wallmark. 1988. Inhibitory effects of cations on the gastric (H, K)-ATPase. *J. Biol. Chem.* 263:10705–10710.

Madeira, V. M. C. 1978. Proton gradient formation during transport of Ca^{2+} by sarcoplasmic reticulum. *Arch. Biochem. Biophys.* 185: 316–325.

Mahaney, J. E., J. F. Froehlich, and D. D. Thomas. 1995. Conformational transitions of the sarcoplasmic reticulum Ca-ATPase studied by time-resolved EPR and quenched-flow kinetics. *Biochemistry.* 34: 4864–4879.

Martell, A. E., and R. M. Smith. 1974. Critical Stability Constants. Plenum Press, New York.

McKinley, D., and G. Meissner. 1978. Evidence for a K^+,Na^+ permeable channel in sarcoplasmic reticulum. *J. Membr. Biol.* 44:159–186.

Miller, C., J. E. Bell, and A. M. Garcia. 1984. The potassium channel of sarcoplasmic reticulum. *Curr. Top. Membr. Transp.* 21:99–132.

Nagel, G., K. Fendler, E. Grell, and E. Bamberg. 1987. Na^+ currents generated by the purified (Na^+-K^+)-ATPase on planar lipid membranes. *Biochim. Biophys. Acta.* 901:239–249.

Navarro, J., and A. Essig. 1984. Voltage-dependence of Ca^{2+} uptake and ATP hydrolysis of reconstituted Ca^{2+} ATPase vesicles. *Biophys. J.* 46:709–717.

Niggli, E., and W. J. Lederer. 1991. Molecular operations of the sodium-calcium exchanger revealed by conformatiom currents. *Nature.* 349: 621–624.

Orlowski, S., and P. Champeil. 1991. Kinetics of calcium dissociation from its high-affinity transport sites on sarcoplasmic reticulum ATPase. *Biochemistry.* 30:353–361.

Petithory, J. R., and W. P. Jencks. 1986. Phosphorylation of the calcium adenosinetriphosphatase of sarcoplasmic reticulum: rate-limiting conformational change followed by rapid phosphoryl transfer. *Biochemistry.* 25:4493–4497.

Petithory, J. R., and W. P. Jencks. 1988. Sequential dissociation of Ca^{2+} from the calcium adenosinetriphosphatase of sarcoplasmic reticulum and the calcium requirement for its phosphorylation by ATP. *Biochemistry.* 27:5553–5564.

Rakowski, R. F., L. A. Vasilets, J. La Tona, and W. Schwarz. 1991. A negative slope in the current-voltage relationship of the Na^+/K^+ pump in *Xenopus* oocytes produced by reduction of external [K^+]. *J. Membr. Biol.* 121:177–187.

Scarpa, A., J. Baldassare, and G. Inesi. 1972. The effect of calcium ionophores on fragmented sarcoplasmic reticulum. *J. Gen. Physiol.* 60:735–749.

Shigekawa, M., and J. P. Dougherty. 1978. Reaction mechanism of Ca^{2+}-dependent ATP hydrolysis by skeletal muscle sarcoplasmic reticulum in the absence of added alkali salts. III. Sequential occurence of ADP-sensitive and ADP-insensitive phosphoenzymes. *J. Biol. Chem.* 253: 1458–1464.

Stengelin, M., K. Fendler, and E. Bamberg. 1993. Kinetics of transient pump currents generated by the (H, K)-ATPase after an ATP concentration jump. *J. Membr. Biol.* 132:211–227.

Sumida, M., and Y. Tonomura. 1974. Reaction mechanism of the Ca^{2+}-dependent ATPase of sarcoplasmic reticulum from skeletal muscle. X. Direct evidence for Ca^{2+} translocation coupled with formation of a phosphorylated intermediate. *J. Biochem.* 75:283–297.

Takisawa, H., and M. Makinose. 1981. Occluded bound calcium on the phosphorylated sarcoplasmic transport ATPase. *Nature.* 290:271–273.

Walker, J. W., G. P. Reid, J. A. McCray, and D. R. Trentham. 1988. Photolabile 1-(2-nitrophenyl)ethylphosphate esters of adenine nucleotide analogues: sythesis and mechanism of photolysis. *J. Am. Chem. Soc.* 110:7170–7177.

Yamada, S., and N. Ikemoto. 1980. Reaction mechanism of calcium-ATPase of sarcoplasmic reticulum. Substrates for phosphorylation reaction and back reaction, and further resolution of phosphorylated intermediates. *J. Biol. Chem.* 255:3108–3119.

Yamaguchi, M., and T. Kanazawa. 1984. Protonation of the sarcoplasmic reticulum Ca-ATPase during ATP hydrolysis. *J. Biol. Chem.* 259: 9526–9531.

Yamaguchi, M., and T. Kanazawa. 1985. Coincidence of H^+ binding and Ca^{2+} dissociation in the sarcoplasmic reticulum Ca-ATPase during ATP hydrolysis. *J. Biol. Chem.* 260:4896–9531.

Yu, X., S. Carrol, J.-L. Rigaud, and G. Inesi. 1993. H^+ countertransport and electrogenicity of the sarcoplasmic reticulum Ca^{2+} pump in reconstituted proteoliposomes. *Biophys. J.* 64:1232–1242.

Yu, X., L. Hao, and G. Inesi. 1994. A pK change of acidic residues contributes to cation countertransport in the Ca-ATPase of sarcoplasmic reticulum. Role of H^+ in Ca-ATPase countertransport. *J. Biol. Chem.* 269:16656–16661.

Zimniak, P., and E. Racker. 1978. Electrogenicity of Ca^{2+} transport catalyzed by the Ca^{2+}-ATPase from sarcoplasmic reticulum. *J. Biol. Chem.* 253:4631–4637.